High precision micro-scale Hall Effect characterization method using in-line micro four-point probes

Petersen, Dirch Hjorth; Hansen, Ole; Lin, Rong; Nielsen, Peter Folmer; Clarysse, T.; Goossens, J.; Rosseel, E.; Vandervorst, W.

Published in:
Proceeding of "IEEE"

Link to article, DOI:
10.1109/RTP.2008.4690563

Publication date:
2008

Document Version
Publisher's PDF, also known as Version of record

16th IEEE International Conference on Advanced Thermal Processing of Semiconductors - RTP2008

High precision micro-scale Hall Effect characterization method using in-line micro four-point probes

D.H. Petersen[a,b], O. Hansen[a,c], R. Lin[b], P.F. Nielsen[b], T. Clarysse[d], J. Goossens[d], E. Rosseel[d], W. Vandervorst[d,e]
[a]DTU Nanotech - Dept. of Micro and Nanotechnology, Technical University of Denmark,
B-345 East, DK-2800 Kgs. Lyngby, Denmark,
[b]CAPRES A/S, Scion-DTU, B-373, DK-2800 Kgs. Lyngby, Denmark,
[c]CINF - Centre for Individual Nanoparticle Functionality, Technical University of Denmark,
B-312, DK-2800 Kgs. Lyngby, Denmark,
[d]IMEC, Kapeldreef 75, B-3001 Leuven, Belgium,
[e]KU Leuven, Dept. of Physics-IKS, Celestijnenlaan 200D, B-3001 Leuven, Belgium
E-mail: dhpe@nanotech.dtu.dk, ohan@nanotech.dtu.dk

Abstract— **Accurate characterization of ultra shallow junctions (USJ) is important in order to understand the principles of junction formation and to develop the appropriate implant and annealing technologies. We investigate the capabilities of a new micro-scale Hall effect measurement method where Hall effect is measured with collinear micro four-point probes (M4PP). We derive the sensitivity to electrode position errors and describe a position error suppression method to enable rapid reliable Hall effect measurements with just two measurement points. We show with both Monte Carlo simulations and experimental measurements, that the repeatability of a micro-scale Hall effect measurement is better than 1 %. We demonstrate the ability to spatially resolve Hall effect on micro-scale by characterization of an USJ with a single laser stripe anneal. The micro sheet resistance variations resulting from a spatially inhomogeneous anneal temperature are found to be directly correlated to the degree of dopant activation.**

Keywords- four-point probe, Hall effect, sheet resistance, dose, mobility, USJ, laser anneal.

I. INTRODUCTION

One of the major challenges for the 32 nm CMOS technology node and beyond is formation of ultra shallow source/drain extensions with very high active dopant concentration and high carrier mobility [1]. In the past, one could safely assume crystalline mobility in many cases when converting sheet resistance to active dopant levels. With more sophisticated processes and structures being developed today (e.g. millisecond anneal, strained Si and SOI), monitoring sheet resistance as well as the degree of dopant activation and carrier mobility in a fast and reliable way is crucial for the understanding of these advanced processes.

Prior experimental work has revealed the need for characterization techniques like the micro four-point probe (M4PP) to accurately characterize sheet resistance of ultra shallow junctions (USJ) [2] with high spatial resolution [3]. Recently, we demonstrated the ability to perform reproducible micro Hall effect measurements to characterize sheet carrier density and mobility of shallow implants in both Si and Ge using M4PP [4]. In a recent comparison between conventional Hall effect methods, Model Based Infra-red spectroscopic Reflectrometry (MBIR) and micro Hall effect measurements, it was found that micro Hall effect measurements seems to give the most reliable results of both sheet resistance, sheet carrier density and carrier mobility when measuring USJ [5].

In this work we demonstrate a new strategy to perform Hall effect measurements with improved measurement precision in less than a minute on unpatterned cleaved wafers with ultra shallow implants. We perform Monte Carlo simulations to investigate the measurement precision and compare this to a repeatability experiment. We then for the first time demonstrate the ability to perform scanning Hall effect measurements with high spatial resolution.

II. THEORY

A. Hall effect measurement

A four-point resistance measurement on a sample is performed by forcing a current, I_0, through two electrodes and simultaneously measuring the potential difference, V, between two other electrodes. In the following we shall consider four-point measurements on a conductive filamentary sheet sample with insulating barriers. Previously, it has been shown that in a moderate magnetic flux density, Hall effect measurements may be performed with a collinear four-point probe in proximity of an insulating barrier, cf. Fig. 1, using two electrode configurations, B and B', where the role of the probe pins are interchanged as illustrated in Figs. 2a and 2b [4].

Two simple definitions become very useful in Hall effect measurements; for resistances measured in configurations B and B', we define the resistance difference, $\Delta R_{BB'} \equiv R_B - R_{B'}$, and the resistance average, $\overline{R_{BB'}} \equiv (R_B + R_{B'})/2$. For an equidistant four-point probe placed parallel to a barrier such as a cleaved edge, the resistance difference is [4]

978-1-4244-1951-7/08/$25.00 ©2008 IEEE

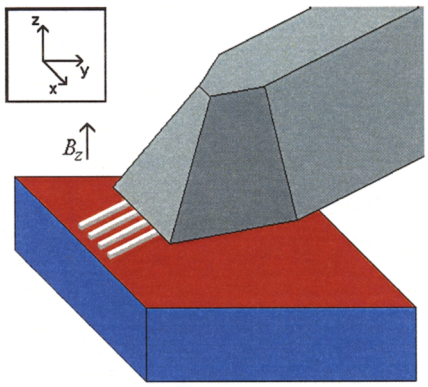

Figure 1. A micro Hall effect measurement is performed with a micro four-point probe (M4PP) positioned in close proximity to an insulating barrier like a cleaved edge.

$$\Delta R_{BB'} = \frac{2R_H}{\pi}\left(3\arctan\left(\frac{s}{2y_0}\right) - \arctan\left(\frac{3s}{2y_0}\right)\right) \quad (1)$$

where R_H is the Hall sheet resistance, s is the electrode pitch and y_0 is the distance between the electrodes and the barrier. The resistance average becomes [4]

$$\overline{R_{BB'}} = \frac{R_0}{2\pi}\left(1+\frac{R_H^2}{R_0^2}\right)\ln(3) + \frac{R_0}{2\pi}\left(1-\frac{R_H^2}{R_0^2}\right)\ln\sqrt{\frac{9+4\left(\frac{y_0}{s}\right)^2}{1+4\left(\frac{y_0}{s}\right)^2}} \quad (2)$$

where R_0 is the direct sheet resistance. Due to symmetry the A and A' configurations, cf. Figs. 2c and 2d, are also interesting since the resistance difference is zero, whereas the resistance average becomes

$$\overline{R_{AA'}} = \frac{R_0}{2\pi}\left(1+\frac{R_H^2}{R_0^2}\right)\ln(4) + \frac{R_0}{2\pi}\left(1-\frac{R_H^2}{R_0^2}\right)\ln\frac{4+4\left(\frac{y_0}{s}\right)^2}{1+4\left(\frac{y_0}{s}\right)^2} \quad (3)$$

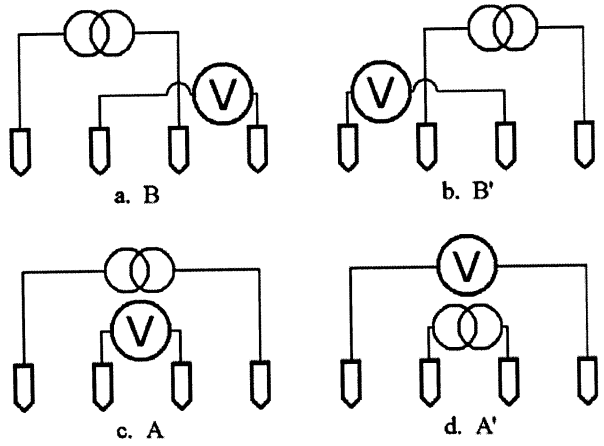

Figure 2. Pin configurations used for Hall sheet resistance and sheet resistance measurements.

The resistance difference, $\Delta R_{BB'}$, can be used to determine the Hall sheet resistance, R_H, while the resistance average can be used to determine the direct sheet resistance, R_0.

B. *Sensitivity to positional errors*

In practical experiments the real positions of the electrodes differ from the ideal positions, and this will affect the measurement precision. Whereas relative position errors between the electrodes may be assumed uncorrelated, the distance between the barrier and the electrodes will result in a correlated position error. Assuming the standard deviations, σ_x and σ_y, of each electrode position are identical for all electrodes, and that the standard deviation on the position of the barrier is σ_b, then the relative standard deviation of $\Delta R_{BB'}$ is [6]

$$\sigma^{rel}_{\Delta R_{BB'}} = \frac{1}{\Delta R_{BB'}}\sqrt{\sum_{N=1}^{4}\left(\left(\frac{\partial \Delta R_{BB'}}{\partial x_N}\right)^2\sigma_x^2 + \left(\frac{\partial \Delta R_{BB'}}{\partial y_N}\right)^2\sigma_y^2\right) + \left(\sum_{N=1}^{4}\frac{\partial \Delta R_{BB'}}{\partial y_N}\sigma_b\right)^2} \quad (4)$$

Based on experience and considerations such as probe positioning accuracy, sample drift and probe tip wear, we assume the magnitude of each position error for a 20 µm pitch M4PP to be σ_x = 500 nm, σ_y = 100 nm and σ_b = 100 nm. The relative standard deviation of the measured resistance difference, $\Delta R_{BB'}$, calculated according to Eq. 4 is then plotted in Fig. 3. The lowest measurement error is found for measurements close to the barrier where the resistance difference is high. Note that for a conventional van der Pauw measurement, the four electrodes are placed on the edge (0 µm from the edge) and the measurement error resulting from the position error σ_x is ideally zero. If the exact position of the probe relative to the barrier can be determined, i.e. σ_b = 0, then the uncertainty of the resistance difference can be reduced to about 0.6 % for a single measurement close to the barrier.

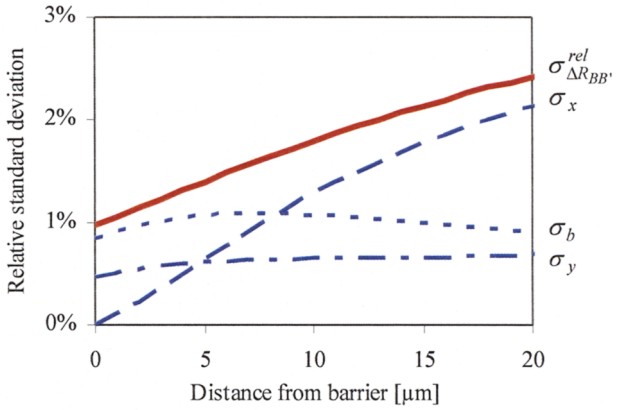

Figure 3. The relative standard deviation of $\Delta R_{BB'}$ measured with a 20 µm pitch M4PP. The relative standard deviation is found by assuming electrode position errors σ_x = 500 nm, σ_y = 100 nm and barrier error σ_b = 100 nm.

C. Position error suppression

The correlated position error, σ_b, can be suppressed if the distance between the probe and the barrier can be determined accurately. To find the average position of the electrodes relative to the barrier and simultaneously extract the sheet resistance, we utilize a dual configuration position correction that is generally used to greatly reduce the effect of electrode position errors on infinite sheets without barriers [7].

$$\exp\left(\frac{2\pi\overline{R_{AA'}}}{R_P}\right)-\exp\left(\frac{2\pi\overline{R_{BB'}}}{R_P}\right)=1 \tag{5}$$

However, due to the presence of the barrier we find a pseudo sheet resistance, R_P, instead of the true sheet resistance. Two pseudo sheet resistance measurements, R_{P1} and R_{P2}, performed with a known distance, Δy, between the measurement positions, may be described as

$$R_{P1}=R_0 f\left(\frac{y_0}{s}\right) \tag{6}$$

$$R_{P2}=R_0 f\left(\frac{y_0+\Delta y}{s}\right) \tag{7}$$

Where R_0 is the direct sheet resistance, y_0 is the position of the barrier, s is the electrode pitch, and the function, f, is implicitly described by Eq. 5. R_0 is eliminated by combining Eqs. 6 and 7.

$$f\left(\frac{y_0}{s}\right)=\frac{R_{P1}}{R_{P2}} f\left(\frac{y_0+\Delta y}{s}\right) \tag{8}$$

Eq. 8 may be solved for y_0 and finally the sheet resistance can be determined by application of Eq. 7. With y_0 determined, the Hall sheet resistance, R_H, is determined by application of Eq. 1. The solution to Eq. 8 is unique if Δy is large enough depending on the value of y_0; if $\Delta y > 1.5s$ the solution is unconditionally unique.

D. Hall carrier mobility and Hall sheet carrier density

The primary parameters measured in a Hall effect measurement are sheet carrier density and carrier mobility. A detailed description of the interpretation of Hall effect measurements may be found elsewhere [4]. The sheet carrier density is determined from

$$N_S = N_{HS}\bar{r}_H = \frac{\bar{r}_H B_z}{ZeR_H} \tag{9}$$

where N_{HS} is the Hall sheet carrier density, Ze is the carrier charge ($Z = \pm 1$), B_z is the magnetic flux density normal to the sample surface and $\bar{r}_H$ is the mean Hall scattering factor. The mean carrier mobility is obtained from

$$\bar{\mu}=\frac{\bar{\mu}_H}{\bar{r}_H}=\frac{ZR_H}{\bar{r}_H R_0 B_z} \tag{10}$$

Here $\bar{\mu}_H$ is the mean Hall carrier mobility. The Hall scattering factor is of order 1 and is dependent on the microscopic details of the carrier momentum relaxation and the carrier distribution function [8].

III. Simulated Measurement Error

In order to assess the potential accuracy of the position error suppression method described above, a Monte Carlo simulation was performed. From Fig. 3 it was found that the uncertainty of the resistance difference was smaller when the four-point probe is placed in close proximity to the barrier. In practical experiments it is difficult to position the electrodes closer than $y_0 = 4$ μm from the barrier because this is done optically. Thus, we choose this position for the measurement of R_{P1}. The position of measurement R_{P2} is then varied to find the best relationship of distance between the measurement positions, Δy, and the measurement uncertainty. For the simulation we apply normal distributed position errors for each electrode position (σ_x = 500 nm and σ_y = 100 nm), a normal distributed position error on the barrier position (σ_b = 100 nm) and a normal distributed resistance measurement error ($\sigma_R = R_0/1.5\times10^5$ Ω). For each Δy, 500 independent simulations were performed for a 20 μm pitch four-point probe.

In Fig. 4 the relative standard deviations of extracted R_0 and R_H are shown as a function of the spatial distance, Δy, between measurements R_{P1} and R_{P2}. From the Monte Carlo simulations it is found that the method for extracting R_0 and R_H eliminates the barrier position uncertainty, σ_b, since the relative standard deviation of R_H is reduced from 1.3 %, cf. Fig. 3, to 0.65 % for $\Delta y > 50$ μm. Furthermore, the relative standard deviation of direct sheet resistance is <0.05 % for $\Delta y > 50$ μm.

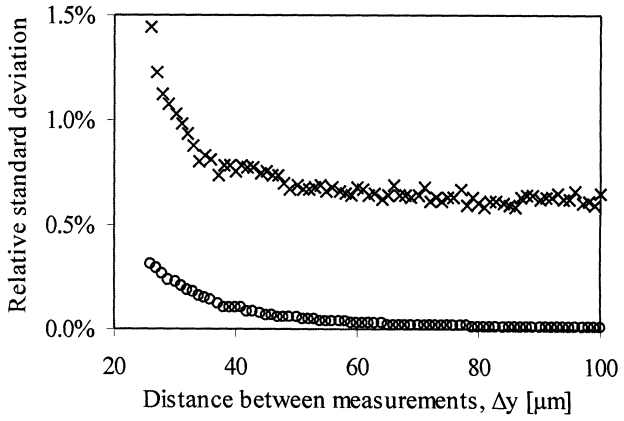

Figure 4. The relative standard deviation of extracted sheet resistance, R_0 (○), and Hall sheet resistance, R_H (×), found from Monte Carlo simulations for a 20 μm pitch four-point probe. Each point is the average of 500 simulations.

The average Hall sheet resistance is found to be underestimated in extracted data from the Monte Carlo simulations by 0.1 % to 0.3 % for $\Delta y > 50$ µm, while the direct sheet resistance is underestimated by <0.01 %. The slightly underestimated direct sheet resistance is expected and is due to the position error in the y-direction, cf. Fig. 1, but the reason for the underestimation of R_H has not been found at this point in time.

IV. Experiments

Micro-scale Hall effect measurements were performed with a micro four-point probe (M4PP) using a CAPRES microRSP-M150 system. The M4PP used in these experiments consists of nickel coated silicon cantilever electrodes extending from the edge of a silicon die. An electrode pitch of 20 µm was chosen for all experiments and the M4PP was equipped with a strain gauge for accurate surface detection. The sample chuck of the microRSP-M150 was fitted with a permanent magnet with a diameter of 35 mm. The resulting magnetic flux density at the position of the samples was on average $B_z = 0.5$ T, but as the magnetic flux density varies slightly across the distances used in the experiments; a custom made Hall sensor, calibrated to within 5 %, was used to determine the field at the exact measurement location (±20 µm). The temperature during measurements was 30.0 ± 0.5 °C.

Prior to measurements, the M4PP is aligned parallel to the cleaved wafer edge, i.e. each tip of the electrodes is positioned at equal distances from the edge. After optical alignment, two pseudo sheet resistance measurements are performed and the exact distance between the edge and the electrodes is calculated. This is done twice at different positions along the edge to account for sample misalignment.

For comparison to the Monte Carlo simulations the position error suppression method is applied by measuring first at a nominal distance of 4 µm to the cleaved edge of a silicon sample and then second at a nominal distance of either 104 µm or 60 µm from the barrier for repeatability measurements and scanning Hall effect experiments, respectively. At both locations the pseudo sheet resistance and resistance difference is measured.

To avoid making assumptions of the Hall scattering factor, the Hall mobility and Hall sheet carrier density will be used instead of drift mobility and sheet carrier density.

V. Results and Discussion

Previously reported micro Hall effect measurements have been performed using a non-linear fitting algorithm to fit multiple measurement points to Eq. 1 [4, 5]. In Figs. 5 and 6, an example is given of 300 pseudo sheet resistance measurements, R_P, and 300 resistance difference measurements, $\Delta R_{BB'}$, which have been measured on a silicon wafer with a sub-melt laser annealed B implant (0.5 keV, 5×10^{14} cm^{-2}). An excellent agreement between experimental results and theory is seen.

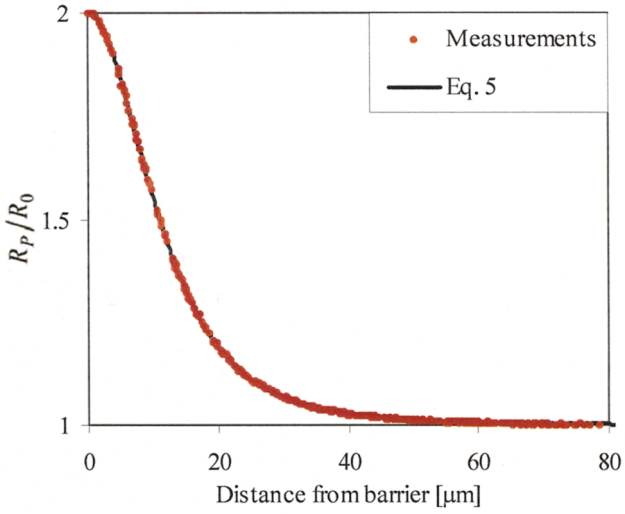

Figure 5. 300 pseudo sheet resistance measurements, R_P, normalized to the direct sheet resistance, R_0. The measurements were performed on a laser annealed USJ with a 20 µm pitch M4PP. The theoretical calculation, Eq. 5, and the experimental results coincide perfectly.

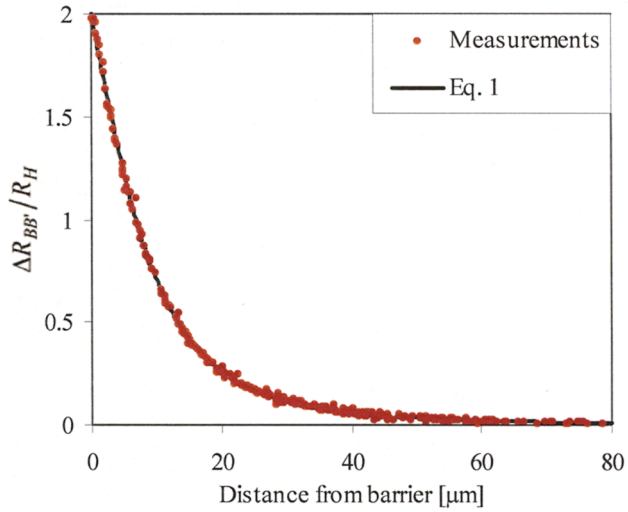

Figure 6. 300 resistance difference measurements, $\Delta R_{BB'}$, normalized to the Hall sheet resistance, R_H. The measurements were performed on a laser annealed USJ with a 20 µm pitch M4PP. The theoretical calculation, Eq. 1, and the experimental results coincide perfectly.

However, such measurements as demonstrated in Figs. 5 and 6 are very time consuming. Thus, the new position error suppression method, that significantly reduces the measurement time needed, is very welcome.

A. Measurement repeatability

To verify the position suppression method experimentally, a repeatability measurement was performed on an RTA annealed silicon wafer with a nominal As dose of 10^{15} cm^{-2} implanted at 2 keV. The wafer was scanned with a 20 µm pitch M4PP along the cleaved edge of the wafer using a step size of 50 µm and performing 50 Hall effect measurements. The measurement results of direct sheet resistance, Hall sheet carrier density and Hall mobility are summarized in Table 1.

TABLE I. VALUES EXTRACTED FROM REPEATABILITY EXPERIMENT.

$R_0 \pm \Delta R_0$	$N_{HS} \pm \Delta N_{HS}$	$\bar{\mu}_H \pm \Delta\bar{\mu}_H$
[Ω]	[$\times 10^{14}$ cm^{-2}]	[cm^{2}V^{-1}s^{-1}]
151.89 ±0.18	6.080 ±0.057	67.60 ±0.58

The relative standard deviation of the measured direct sheet resistance, R_0, and Hall sheet resistance, R_H, is 0.12 % and 0.94 %, respectively. This is higher than predicted in the Monte Carlo simulations, i.e. 0.05 % and 0.65 %, respectively. These differences could be the result of the position of first measurement being different from the nominal 4 µm, cf. the sensitivity plot Fig. 3. However, since the average and standard deviation of the calculated position of the first measurement point, R_{P1}, from the barrier was y_0 = 4.30 ±0.45 µm, it is more likely due to an under estimated position error in the y-direction, i.e. σ_y > 100 nm. Nevertheless, the relative standard deviations are lower than those we have reported earlier [4, 5] and the agreement between Monte Carlo simulation and experiment is reasonably good.

To further reduce the error arising from uncorrelated position errors, static contact M4PP with high aspect ratio L-shaped cantilevers may be useful since position repeatability better than 11 nm has previously been reported [6]. Also, since the sensitivity of both R_0 and R_H to position errors depends on the choice of probe pitch, a slightly larger probe pitch may be used in order improve accuracy, but that will reduce the spatial resolution to resistance variations [3].

B. *Scanning Hall effect*

In addition to the improved measurement accuracy the position error suppression method significantly reduces the measurement time to less than a minute, i.e. 10-30 times faster than the results reported in previous publications [4, 5]. The reduced measurement time allows for scanning Hall effect measurements to investigate the cause of spatial sheet resistance variations seen for laser annealed USJ. To explore the scanning capability, a silicon wafer with a nominal B dose of 10^{15} cm^{-2} was exposed to a scanning sub-melt laser anneal by performing a single pass of an 11 mm wide laser spot. For convenience we define the direct sheet conductivity, G_0, as

$$G_0 = R_0^{-1} = e\bar{\mu}N_S = e\bar{\mu}_H N_{HS} \qquad (11)$$

The annealed region of the wafer was then characterized and the result is summarized in Fig. 7, where the relative Hall carrier mobility, the relative Hall sheet carrier density and the relative sheet conductivity is plotted. For this scan the average and standard deviation of the calculated position of the first measurement point, R_{P1}, was y_0 = 4.22 ±0.76µm. The slightly higher standard deviation of the position of the first measurement point as compared to ±0.45 µm for the RTA annealed sample may be an indication that the position error suppression is less accurate for samples with micro-scale inhomogeneous sheet resistance.

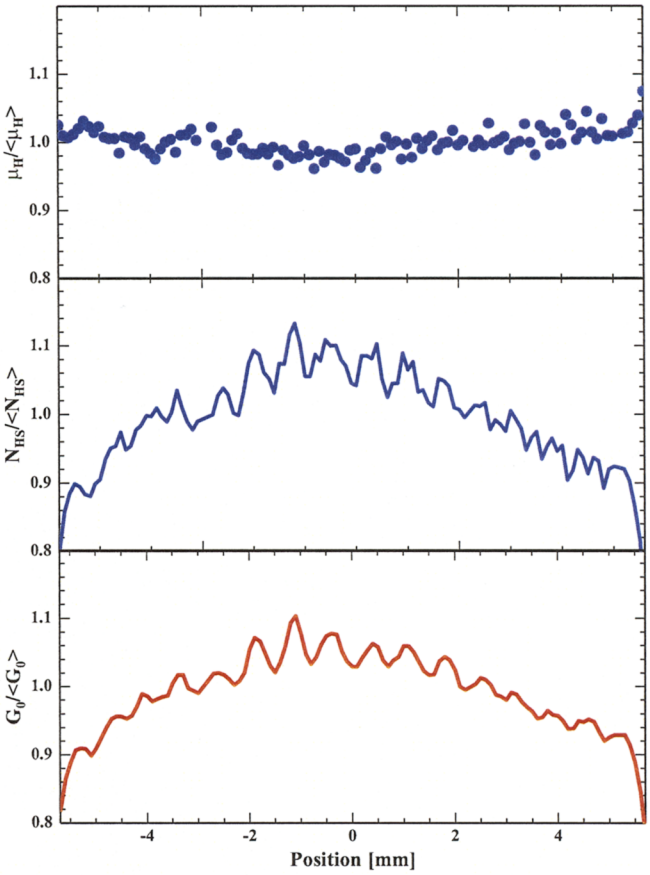

Figure 7. Scanning Hall effect measurement of a silicon sample with an ultra shallow boron implant. The sample was laser annealed in a single pass of an 11 mm wide laser beam. Hall mobility and Hall sheet carrier dose and sheet conductance are each normalized by their respective average value. The measurement time was less than a minute per point.

The result is, as one would expect, an almost perfect correlation between active dose and sheet conductance, since the carrier mobility only has a weak dependence on the active dopant concentration in highly doped material. The slight decrease in Hall mobility seen at higher activation degree could be an indication of increased carrier scattering from ionized impurities, i.e. substitutional B atoms rather than interstitial defects.

To evaluate the micro Hall effect measurement precision on this inhomogeneous sample, we calculate the standard deviation of Hall carrier mobility which according to both theory and Fig. 7 should be the parameter with the smaller dependency on sample variations. For this evaluation we restrict the calculation to the period [-2 ; 2] mm with stable mobility and find the relative standard deviation to be 1.3 %. It may then be reasonable to assume that the relative uncertainty of the measured Hall carrier mobility and Hall sheet carrier density is equal to or better than 1.3 % on this inhomogenous sample while excluding the absolute uncertainty (<5 %) of the magnetic flux density.

VI. Conclusion

We have investigated the precision of a new micro Hall effect measurement method based on measurements with a collinear M4PP near an edge. We calculated the relative standard deviation of the resistance difference, $\Delta R_{BB'}$, and found that the measurement error on $\Delta R_{BB'}$ is lower when performed close to an edge and mainly determined by the uncertainty on the distance, y_0, between the M4PP and the edge. We described a position error suppression method based on measurements at just two positions to reduce the uncertainty on y_0. The position error suppression method was applied first in a Monte Carlo simulation and then in a repeatability experiment; and we find the relative standard deviation of measurement repeatability to be less than 1 % for both simulations and measurements.

Furthermore, we demonstrated spatially resolved scanning micro Hall effect measurements on laser annealed USJ with spatial sheet resistance variations. We find an almost perfect correlation between the active dose and the sheet conductance (inverse sheet resistance), while in regions with low sheet resistance variations the carrier mobility is almost constant. Finally, we find that even for a sample with significant spatial variations in sheet resistance on the order of 5 % a relative standard deviation of less than 1.3 % in micro Hall effect measurements may be expected excluding the absolute uncertainty of the magnetic flux density.

Acknowledgment

We are grateful for the financial support from Copenhagen Graduate School for Nanoscience and Nanotechnology C:O:N:T, the Danish Research Agency FTP. Center for Individual Nanoparticle Functionality (CINF) is sponsored by The Danish National Research Foundation. We thank Peter Bøggild for continuous support, encouragement, and fruitful discussions.

References

[1] International Technology Roadmap for Semiconductors, http://www.itrs.net.

[2] T. Clarysse, A. Moussa, F. Leys, R. Loo, W. Vandervorst, M. C. Benjamin, R. J. Hillard, V. N. Faifer, M. I. Current, R. Lin, and D. H. Petersen, Mater. Res. Soc. Symp. Proc. 912, 197 (2006).

[3] D. H. Petersen, R. Lin, T. M. Hansen, E. Rosseel, W. Vandervorst, C. Markvardsen, D. Kjær, and P. F. Nielsen, J. Vac. Sci. Technol. B 26, 362 (2008).

[4] D. H. Petersen, O. Hansen, R. Lin, and P. F. Nielsen, J. Appl. Phys. 104, 013710 (2008).

[5] T. Clarysse, J. Bogdanowicz, J. Goossens, A. Moussa, E. Rosseel, W. Vandervorst, D.H. Petersen, R. Lin, P.F. Nielsen, O. Hansen, G. Merklin, N.S. Bennett and N.E.B. Cowern, "On the analysis of the activation mechanisms of sub-melt laser anneals", European Material Research Society Spring meeting, Strasbourg, 26-30 May 2008, Symposium I, (to be published in Materials Science and Engineering B).

[6] D. H. Petersen, O. Hansen, T. M. Hansen, P. R. E. Petersen and P. Bøggild, Microelectron. Eng. 85, 1092 (2008).

[7] R. Rymaszew, J. Phys. E: J. Sci. Instrum. 2, 170 (1969).

[8] K. Seeger, Semiconductor Physics, An Introduction, Solid-State Sciences No. 40, 5th ed. (Springer, Berlin, 1991).